

## **Structural response of timber-concrete composite beams predicted by finite element models and manual calculations**

\*Nima Khorsandnia<sup>1)</sup>, Hamid R. Valipour<sup>2)</sup> and Keith Crews<sup>3)</sup>

<sup>1), 3)</sup> *Centre for Built Infrastructure Research (CBIR), School of Civil and Environmental Engineering, University of Technology, Sydney, P.O.Box123 Broadway, NSW, Australia*

<sup>2)</sup> *Centre for Infrastructure Engineering and Safety (CIES), School of Civil and Environmental Engineering, The University of New South Wales, Sydney, Australia*

<sup>1)</sup> *Nima.Khorsandnia@uts.edu.au*

### **ABSTRACT**

This paper presents a comparative study of the structural response of timber-concrete composite (TCC) beams predicted by finite element models (i.e. continuum-based and 1D frame) and manual calculations. Details of constitutive laws adopted for modelling timber and concrete are provided and application of the Hashin damage model in conjunction with continuum-based FE for capturing failure of timber under bi-axial stress state is discussed. A novel strategy for modelling the TCC connection is proposed in which the connection is modelled by a nonlinear spring and the full load-slip behaviour of each TCC connection is expressed with a formula that can be directly implemented in the general purpose FE codes and used for nonlinear analysis of TCC beams. The developed FE models are verified by examples taken from the literature. Furthermore, the load-displacement response and ultimate loading capacity of the TCC beams are determined according to Eurocode 5 method and compared with FE model predictions.

### **1 INTRODUCTION**

Timber–concrete composite (TCC) beams have higher stiffness, ultimate loading capacity and fire rating compared to timber beams. Furthermore, under service loads TCC floors have less deflection and vibration and can provide more effective diaphragm action compared to floors made solely from timber. Accordingly, TCC members have found increased usage over the last twenty years and extensive research has been devoted to experimental, numerical and analytical studies as well as development of simplified methods and design provisions for TCC beams (Ahmadi & Saka 1993; Ceccotti 1995; Ceccotti et al. 2006; Clouston et al. 2005; Lopes et al. 2012).

The experimental studies undertaken by different research groups cover various

---

<sup>1)</sup> PhD Candidate

<sup>2)</sup> Senior Lecturer

<sup>3)</sup> Professor

Note: Copied from the manuscript submitted to “Structural Engineering and Mechanics, An International Journal” for presentation at ASEM13 Congress

local and global aspects of TCC systems. At local (joint or connection) level, behaviour of different types of connections (Branco et al. 2009; Deam et al. 2008; Gutkowski et al. 2004; Steinberg et al. 2003) and developing new connections with higher level of composite action (Clouston et al. 2004; Fragiaco et al. 2007; Yeoh et al. 2011a) have been investigated and at global level application of different timber products (i.e. LVL, sawn timber and glulam) (Balogh et al. 2008; Clouston et al. 2005; Gutkowski et al. 2008; Yeoh et al. 2011b), using different classes of concrete or developing new construction methods for the slabs (Brunner et al. 2007; Jorge et al. 2011; LeBorgne & Gutkowski 2010; Lukaszewska et al. 2008), ultimate loading capacity of the TCC beams under short-term loads and long-term behaviour of TCC systems (Ceccotti et al. 2006; Fragiaco 2005, 2012) have been studied by different researchers.

The numerical studies focus on application of FE models for capturing the local response of TCC joints (Dias et al. 2007a; Schäfers & Seim 2011) and global response of the TCC beams (Gutkowski et al. 2010; Lopes et al. 2012). Timber-concrete composite beams can be analysed using either continuum-based finite element models or 1D discrete frame elements. Typically, in the 1D frame models the section is discretized into fibres (filaments) and only behaviour of material under a uniaxial stress state can be captured (Lukaszewska et al. 2010; Valipour & Bradford 2009). Accordingly, the frame FE models are mainly applicable for capturing the global response of TCC beams whereas the continuum-based FE models can capture the global and local response of TCC beams and joints with good accuracy (Dias et al. 2007b; Gutkowski et al. 2010).

The simplified analytical models are typically derived from the solution of governing differential equation of the simply supported TCC beams by assuming a linear elastic behaviour for timber, concrete and connections (CEN 2008; Clouston et al. 2005). In addition, some attempts have been made to formulate the behaviour of mechanical fasteners using beam on elastic foundation theory (Gelfi et al. 2002).

For nonlinear analysis of TCC beams using continuum-based FE models, the timber beam and concrete slab are divided to small brick or membrane elements and the bond between concrete and timber is usually modelled by a contact element (Dias et al. 2007b; Schäfers & Seim 2011). However, the normal and tangential stiffness of existing contact elements are typically linear and therefore cannot sufficiently represent the nonlinear behaviour of discrete mechanical fasteners (such as nails & screws) in TCC systems. Furthermore, the loading capacity of the typical interface elements are formulated based on elastic/rigid-perfect plastic behaviour according to Columb or modified Columb friction models (*ABAQUS* 2011; *ANSYS* 2011) that warrants a prior calibration of the input parameters (i.e. cohesion and coefficient of friction) without having direct relevance to the real behaviour of discrete mechanical fasteners.

In this paper the nonlinear short-term structural response of TCC beams is captured by three different models (viz. continuum-based FE, 1D frame fibre element and manual calculation according to Eurocode 5 provisions). Further, a novel strategy for modelling TCC connections is proposed in which the fastener is modelled by a nonlinear spring. In the proposed approach, the full load-slip response of the connector can be directly incorporated into the FE model to predict the load-displacement response of TCC beams including their ultimate loading capacity. A comparative study is undertaken to verify the accuracy and demonstrate the merits of each model.

## 2 FINITE ELEMENT MODELLING OF TCC BEAMS

### 2.1 Continuum-based finite element model

#### Application of Hashin failure criteria for modelling timber

From the mechanical point of view, timber is anisotropic material with different behaviours along the grain and perpendicular to the grain direction (Mackenzie-Helwein et al. 2003). In the developed 2D continuum-based FE models, the nonlinear behaviour of timber is captured by Hashin damage criteria (Hashin 1980; Hashin & Rotem 1973). The Hashin damage model takes account of interaction between shear and normal stress components to evaluate different failure modes. The Hashin damage model was originally developed for unidirectional polymeric composites (Hashin 1980; Hashin & Rotem 1973), and hence, application to other laminate types or non-polymeric composites represents a significant approximation. In this study, however, it is shown that Hashin model can adequately capture the failure modes of timber under bi-axial stress states, particularly within the timber and timber-concrete composite beams. The accuracy of Hashin model has been verified by experimental results including timber beams with and without notches and holes subject to three and four-point bending tests (Khorsandnia et al. 2013). The 2D Hashin failure criteria adopted in this study are used to predict the onset of damage, and the damage evolution law is based on the energy dissipated during the damage process and linear material softening (ABAQUS 2011). The 2D Hashin criteria considers four different damage initiation mechanisms expressed in terms of effective stress components  $\hat{\sigma}_{ij}$  ( $i, j = 1, 2$ ), as follows

$$\left\{ \begin{array}{l} F_f^t = \left( \frac{\hat{\sigma}_{11}}{X^T} \right)^2 + \alpha \left( \frac{\hat{\sigma}_{12}}{S^L} \right)^2 \\ F_f^c = \left( \frac{\hat{\sigma}_{11}}{X^C} \right)^2 \\ F_m^t = \left( \frac{\hat{\sigma}_{22}}{Y^T} \right)^2 + \alpha \left( \frac{\hat{\sigma}_{12}}{S^L} \right)^2 \\ F_m^c = \left( \frac{\hat{\sigma}_{22}}{2S^T} \right)^2 + \left[ \left( \frac{Y^C}{2S^T} \right)^2 - 1 \right] \left( \frac{\hat{\sigma}_{22}}{Y^C} \right) + \left( \frac{\hat{\sigma}_{12}}{S^L} \right)^2 \end{array} \right. \quad \begin{array}{l} : \text{Tensile failure of fibers} \\ : \text{Compression failure of fibers} \\ : \text{Tensile failure of matrix} \\ : \text{Compression failure of matrix} \end{array} \quad (1)$$

where  $X^T$  and  $Y^T$  are the tensile strength of timber along the grain and perpendicular to grain, respectively,  $X^C$  and  $Y^C$  are the compressive strength of timber along the grain and perpendicular to grain, respectively,  $S^L$  and  $S^T$  denote the shear strength along the grain and perpendicular to grain, respectively, and  $\alpha$  is a coefficient that determines the contribution of the shear stress to the fibre tensile initiation criterion.

The effective stress vector  $\hat{\boldsymbol{\sigma}} = [\hat{\sigma}_{11} \ \hat{\sigma}_{22} \ \hat{\sigma}_{12}]^T$ , is related to stress vector

$$\boldsymbol{\sigma} = [\sigma_{11} \quad \sigma_{22} \quad \sigma_{12}]^T \text{ by} \quad \hat{\boldsymbol{\sigma}} = \boldsymbol{\omega} \boldsymbol{\sigma} \quad (2)$$

in which,  $\boldsymbol{\omega}$  is a damage matrix defined as follows

$$\boldsymbol{\omega} = \begin{bmatrix} 1/(1-\omega_f) & 0 & 0 \\ 0 & 1/(1-\omega_m) & 0 \\ 0 & 0 & 1/(1-\omega_s) \end{bmatrix} \quad (3)$$

where  $\omega_f$  and  $\omega_m$  are scalar damage variables for fibres and matrix, respectively, and  $\omega_s$  is shear damage variable expressed as a function of  $\omega_f$  and  $\omega_m$  (ABAQUS 2011).

### Modelling concrete using a plastic-damage constitutive law

In the developed FE models, a plastic-damage constitutive law is adopted for concrete (Lubliner et al. 1989). The incremental stress-strain relationship of the adopted model is cast in the formwork of isotropic damage and governed by

$$\boldsymbol{\sigma} = (1 - \omega) \mathbf{D}_0^{\text{el}} (\boldsymbol{\varepsilon} - \boldsymbol{\varepsilon}^{\text{pl}}) \quad (4)$$

where  $\mathbf{D}_0^{\text{el}}$  is the initial (undamaged) elastic stiffness of the material,  $\boldsymbol{\varepsilon}^{\text{pl}}$  is plastic strain and  $\omega$  is the scalar damage variable that captures the stiffness degradation of material. It should be noted that damage associated with the failure mechanisms of the concrete (cracking and crushing) leads to a reduction in the elastic stiffness of material. Further details on yield surface, flow rule and hardening law of the adopted plastic-damage model can be found in Lee and Fenves (1998).

The modulus of elasticity of concrete is a function of compressive strength and typically varies between  $5000\sqrt{f_{cp}}$  and  $1000f_{cp}$  (MPa) in different standards and therefore, an average value is adopted in this method.

### Modelling the TCC connections

In the finite element modelling of TCC beams, the connection between timber beam and concrete slab is usually modelled by contact elements (Dias et al. 2007b; Mascia & Soriano 2004; Schäfers & Seim 2011). The available contact elements are typically characterised by five parameters including normal stiffness of interface  $K_{nn}$ , tangential stiffness of interface  $K_{tt}$ , cohesion  $c$ , coefficient of friction  $\phi$  and tensile strength  $f_t$  of the interface. The normal and tangential stiffness of contact elements are linear elastic up to failure point and therefore the existing interface elements can only capture the linear elastic-brittle failure behaviour (Fig. 1), which is not consistent with the real behaviour of TCC connections (normal screws, SFS, etc) observed during testing.

With regard to the lumped nature of mechanical fasteners used in TCC connections, in this study a simple modelling technique is proposed that can adequately capture the

nonlinear behaviour of connections. In this modelling strategy, the concrete slab and timber beams are generated and meshed as two separate objects and some selected nodes from timber beams are horizontally constrained to nodes within the concrete slab by equivalent nonlinear springs which represent the mechanical fasteners (Fig. 2). In the vertical direction, the interfacial nodes from concrete slab and timber beams are fully constrained to prevent possible penetration of contacting objects (see Fig. 2). The proposed modelling strategy has two advantages. First, the nonlinear shear-slip response of the connections can be directly incorporated into the FE formulation, which is more consistent with the real behaviour of TCC connections and improves the accuracy of FE model. Second, the proposed modelling strategy does not need a prior calibration of input parameters as opposed to normal contact elements.

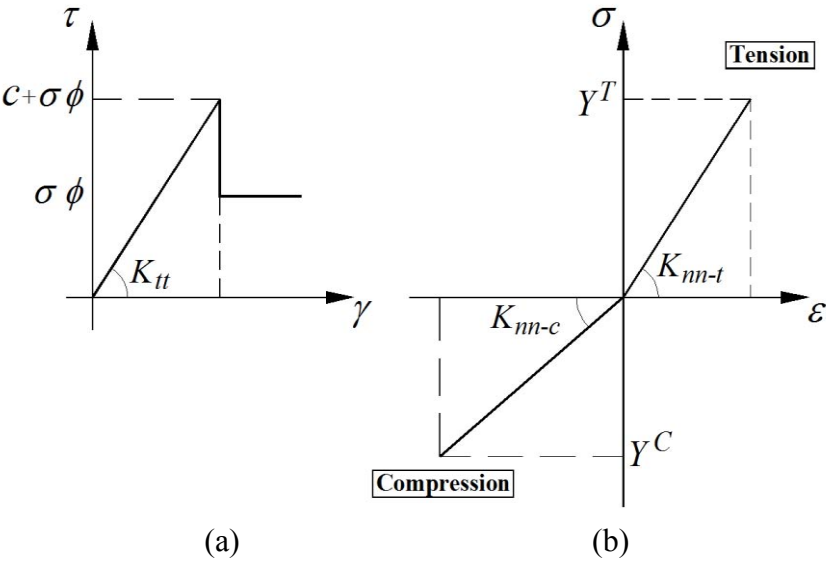


Fig. 1 Typical interface model behaviour under (a) tangential (b) normal (tension/Compression) stresses.

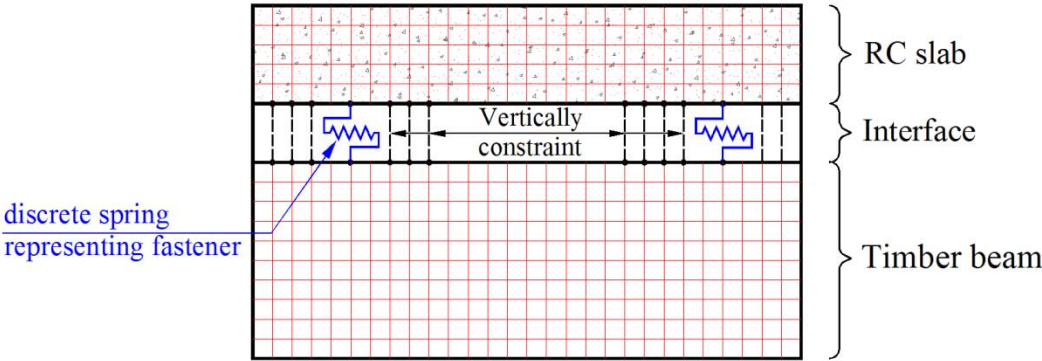


Fig. 2 Schematic outline of the continuum-based FE mesh and interface between RC slab and timber beam.

The shear-slip behaviour of equivalent springs representing TCC connections can be characterised using a curve fitting or nonlinear regression technique. Depending on the connection type (e.g. normal screw, SFS, notches etc) and the functions adopted for regression, different models can be developed (Khorsandnia et al. 2012; Yeoh et al. 2011a). For example, the pre-peak response (ascending part) of the shear-slip ( $P$  versus  $s$ ) diagram for normal screw connection can be adequately represented by the Richard-Abbott model (Khorsandnia et al. 2012; Valipour & Bradford 2013)

$$P = \frac{(k_0 - k_p)|s|}{\left[1 + \left|\frac{(k_0 - k_p)|s|}{P_0}\right|^n\right]^{\frac{1}{n}}} + k_p|s| \quad (5)$$

where  $k_0$  is the initial stiffness,  $k_p$  is the strain-hardening stiffness,  $P_0$  is a reference shear force and  $n$  is a parameter which controls the curvature of the diagram (Fig. 3a).

In addition, the ascending part of the shear-slip behaviour for SFS and notch connections can be respectively modelled by the exponential function (Khorsandnia et al. 2012) and Ollgard's model (Ollgard et al. 1971) as follows

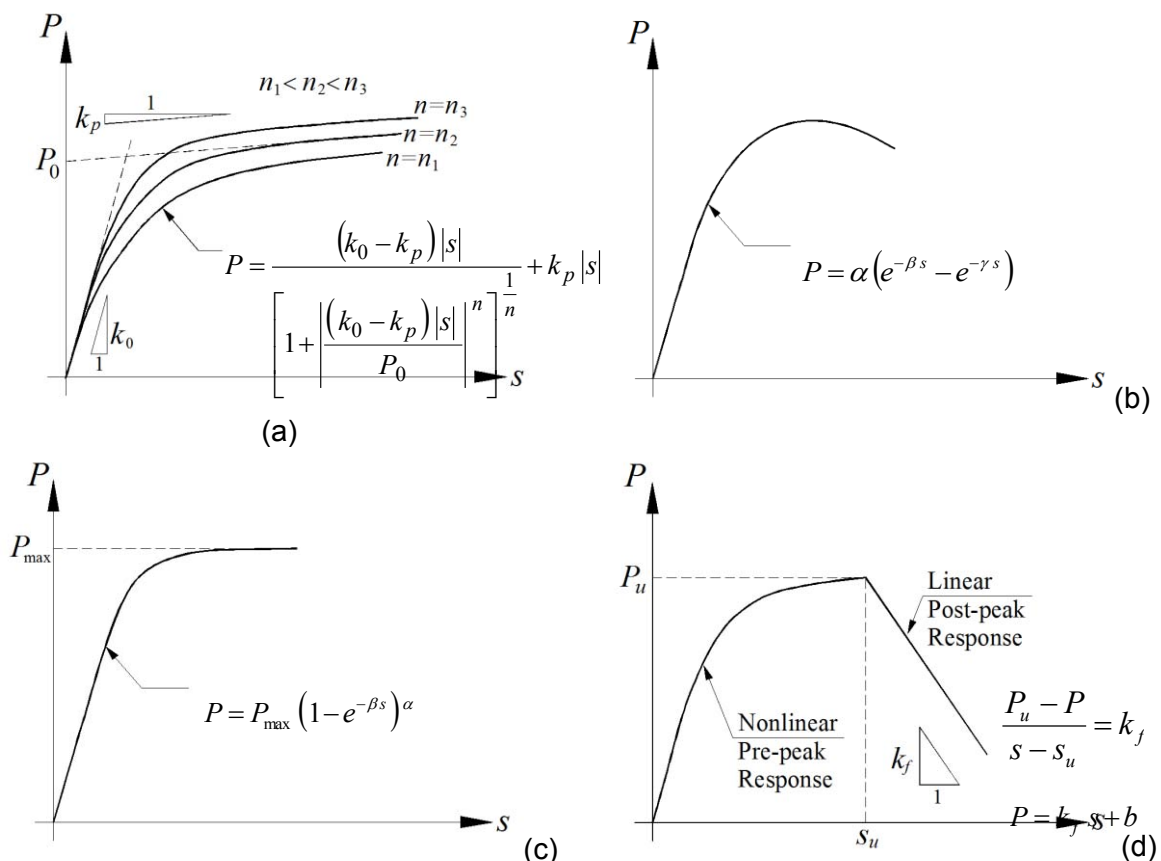


Fig. 3 Schematic outline of the (a) Richard-Abbott model (b) Exponential model (c) Ollgard model (d) Pre-peak and Post-peak responses for TCC connections.

$$P = \alpha \left( e^{-\beta s} - e^{-\gamma s} \right) \quad (6)$$

$$P = P_{\max} \left( 1 - e^{-\beta s} \right)^\alpha \quad (7)$$

where  $P_{\max}$  represents the maximum shear strength of the connection and  $\alpha$ ,  $\beta$ ,  $\gamma$  are parameters which control the curvature of function (Fig. 3b,c). Regarding the post-peak (softening) part of the shear-slip diagrams, typically a linear function (see Fig. 3d) is adequate (Khorsandnia et al. 2012; Yeoh et al. 2011a).

In this study, seven different connections including normal screw, SFS, notch and screw have been chosen from literature and their pre-peak and post-peak responses are categorized and reported in Table 1. The 'NS' is a normal wood screw with a length of 100 mm and 5 mm diameter. The 'SFS' comprises two inclined screws with a length of 200 mm specifically designed for application in TCC beams. The 'BM' and 'T' are bird mouth connections with a triangular notch reinforced with 16 mm diameter coach screw. Further, the 'R150' and 'R300' connections represent triangular notch with 150 and 300 mm length, respectively, reinforced with 16 mm diameter lag screw. 'Steel Mesh' is a continuous connection with one half glued into a slot in timber and the other half embedded in concrete.

Table 1. Pre-peak, post-peak and semi-composite stiffness of TCC connections used in FE models and manual analysis.

Connection Type	Pre-peak Response				Post-peak Response		K for semi-comp. (kN/mm)		
	Model	Parameters			Model	Parameters			
NS (Khorsandnia et al. 2012)	Richard-Abbott	$P_0$	$k_0$	$k_p$	$n$	Linear	$k_f$	$b$	$K_{s,0.6}$
		8.02	68.03	0.42	0.61		-2.8	36.3	7.1
SFS (Khorsandnia et al. 2012)	Exponential	$\alpha$	$\beta$	$\gamma$		Linear	$k_f$	$b$	$K_{s,0.4}$
		328.88	-0.31	-0.40			-29.9	152.1	54.9
BM (Khorsandnia et al. 2012)		$P_{\max}$	$\alpha$	$\beta$			$k_f$	$b$	$K_{s,0.4}$
		56.57	2.28	1.41			-5.7	95.6	36.9
R150 (Yeoh et al. 2011a)	Ollgard					Linear			
		80.00	1.40	3.55			-5.8	90.0	164.2
R300 (Yeoh et al. 2011a)		134.41	1.40	3.55			-5.8	151.6	275.9
T (Yeoh et al. 2011a)		89.92	1.12	2.48					
Steel Mesh (Clouston et al. 2005)		110.90	1.06	5.59					

## 2.2 1D frame fibre element

In the 1D frame element models, reinforced concrete (RC) slab and timber beam are modelled by two separate frame elements which are coupled by discrete nodal springs in the longitudinal direction (see Fig. 4) and the stiffness (viz. force-displacement relationship) of these longitudinal springs can be directly extracted from the shear-slip response of TCC connection as described in previous section. In the transverse direction, RC slab and timber beam are rigidly constrained assuming that separation between slab and beam is negligible. Moreover, the section of RC slab as well as timber beam is sub-divided into fibres (layers in 2D) that allows for monitoring the behaviour of material points over the section depth (Valipour & Bradford 2012).

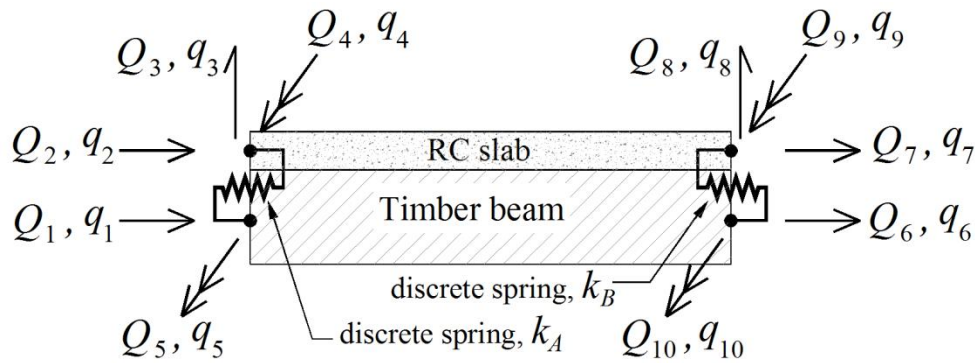


Fig. 4 Coupling of reinforced concrete (RC) slab and timber beam using longitudinal nodal springs ( $q$  and  $Q$  are generalised nodal displacements and forces, respectively).

### Constitutive law for timber

In the typical fibre element models, effect of shear on the nonlinear response of material is neglected; accordingly a uniaxial material law can adequately model the nonlinear behaviour of timber properties parallel to grain (along the beam axis). Among the various available uniaxial constitutive laws for timber in compression (Connors 1989), the stress-strain law presented by Glos (1981), which originally has been developed for small clear timber specimens, is adopted in this study (Fig. 5a),

$$\sigma = \begin{cases} \frac{\varepsilon + \alpha_1 \varepsilon^n}{\alpha_2 + \alpha_3 \varepsilon + \alpha_4 \varepsilon^n} & \text{for } -\varepsilon_u \leq \varepsilon \leq 0 \\ 0 & \text{for } \varepsilon < -\varepsilon_u \end{cases} \quad (8)$$

$$\alpha_1 = \frac{100 f_{cy}}{(n-1) E_0 \varepsilon_0^{(n-1)} (1 - f_{cy}/f_{cu})}, \quad f_{cy} \leq f_{cu} - 1 \text{ (MPa)} \quad (9)$$

$$\alpha_2 = \frac{1}{E_0}, \quad \alpha_3 = \frac{1}{f_{cu}} - \frac{n}{(n-1) E_0 \varepsilon_0}, \quad \alpha_4 = \frac{\alpha_1}{f_{cy}}$$



where,  $f_{cu}$  and  $\varepsilon_0$  are the ultimate compressive strength and corresponding strain, respectively,  $f_{cy}$  is the residual stress,  $E_0$  is the initial elastic modulus of timber in compression and  $n$  is a shape parameter which controls the curvature (see Fig. 5a). The typical values adopted for the input parameters in the Glos model (1981) are:  $f_{cy} = 0.8f_{cu}$ ,  $\varepsilon_0 = 0.008-0.012$  and  $\varepsilon_u \approx 3\varepsilon_0$ .

Tension behaviour of timber follows a linear elastic part up to tensile strength  $f_{tu}$ , and after that the material softens linearly (see Fig. 5a). The slope of the softening branch is characterised and adjusted by assuming a constant fracture energy density  $G_f$ , that serves as a localisation limiter.

### Constitutive law for concrete

In 1D frame fibre element models, a uniaxial stress-strain relationship based on the CEB-FIP model code 1990 (CEB-FIP 1993) is used for concrete under compression and tensile concrete follows a linear elastic-quasi brittle failure model with an exponential softening curve (Fig. 5b). The strain corresponding with maximum stress for compressive concrete is  $\varepsilon_{c0} = 0.002$  and ultimate strain of concrete is  $\varepsilon_{cu} = 0.01$  (Fig. 5b). Further, for unloading/reloading regime a damage model with no plastic strain is adopted in this study (Fig. 5b).

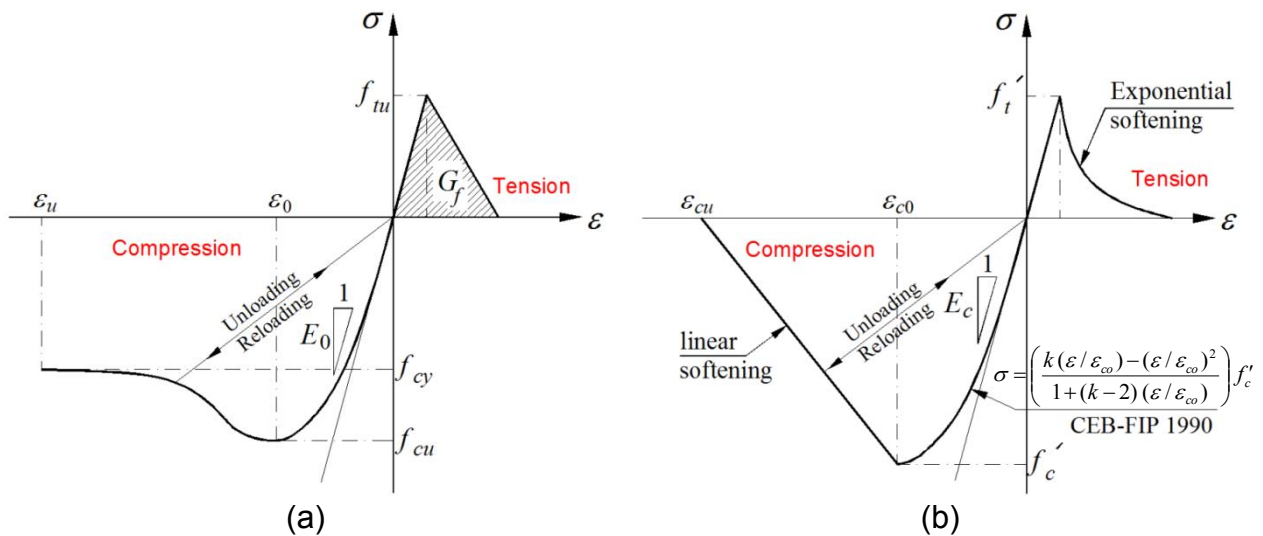


Fig. 5 Schematic outline of the adopted stress-strain relationship for (a) timber (b) concrete.

## 3 MANUAL ANALYSIS ACCORDING TO EUROCODE 5 PROVISIONS

This method is based on direct fulfilment of strain-displacement compatibility and static equilibrium equations of composite sections. Using manual calculations the full-composite, semi-composite and no-composite action as well as behaviour of timber beam alone can be captured.

In the full-composite case, it is assumed that no slip between timber and concrete

occurs and flexural stiffness  $EI_{fc}$  for the full-composite T-sections can be obtained from

$$EI_{fc} = E_c I_c + E_c A_c a_1^2 + E_t I_t + E_t A_t a_2^2 \quad (10)$$

where subscript  $c$  and  $t$  represents concrete and timber, respectively,  $E$  denotes material modulus of elasticity and  $A$  and  $I$  denote the cross-sectional area and the second moment of the area for each section, respectively (i.e. concrete and timber) about their reference axis (see Fig. 6).  $h_c$  and  $h_t$  denote thickness of concrete slab and depth of timber beam as shown in Fig. 6 and

$$a_2 = \frac{E_c A_c (h_c + h_t)}{2(E_c A_c + E_t A_t)}, \quad a_1 = \frac{h_c + h_t}{2} - a_2 \quad (11)$$

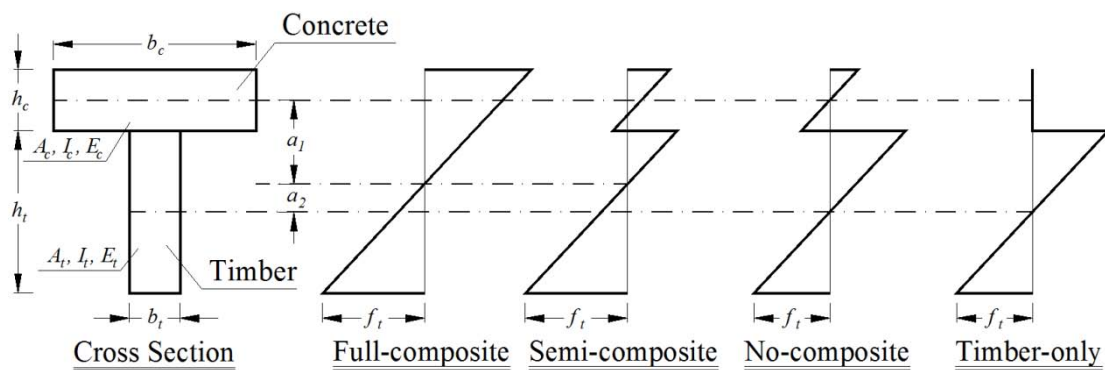


Fig. 6 TCC cross-section and schematic distribution of bending stresses in different cases.

The semi-composite case is based on the partial interaction between timber beam and concrete slab which are coupled by connections (e.g. chemical bond, mechanical fastener or combination of both). In manual calculations the fasteners are characterised by their slip modulus  $K$  (assuming a linear response) and spacing  $S$  between them (equally spaced). Most of the aforementioned connections show almost linear behaviour before failure and therefore, the linear stiffness ( $K$ ) in this method can be assumed to be the same as serviceability slip modulus ( $K_{s,0.4}$ ) according to European Standard (CEN 1991). Since there is a significant nonlinearity in shear-slip response of „NS’ connection, the ultimate slip modulus ( $K_{s,0.6}$ ) seems to be more appropriate for capturing the global response of the TCC beam. The magnitude and type of stiffness adopted for manual analysis of each and every one of the connections considered in this study are given in Table 1. Further, the fasteners spacing,  $S$ , is also calculated based on the equally spaced distribution of the connections over the beam length. The deflection of a simply supported semi-composite TCC beam with span length  $L$  can be calculated by using an effective flexural stiffness  $EI_{ef}$  given in Eurocode 5, Annex B (CEN 2008) as follows

$$EI_{ef} = E_c I_c + \gamma_1 E_c A_c a_1^2 + E_t I_t + E_t A_t a_2^2 \quad (12)$$

Where

$$a_2 = \frac{\gamma_1 E_c A_c (h_c + h_t)}{2(\gamma_1 E_c A_c + E_t A_t)}, \quad \gamma_1 = \frac{1}{1 + \frac{\pi^2 E_c A_c S}{K L^2}}, \quad a_1 = \frac{h_c + h_t}{2} - a_2 \quad (13)$$

In the no-composite case, the horizontal shear is not transferred on the interface between timber and concrete slab and the total bending stiffness of the member  $EI_{nc}$  in such a case is obtained from

$$EI_{nc} = E_c I_c + E_t I_t \quad (14)$$

Finally, in the timber-only case it is assumed that there is no concrete slab on top of the timber beam and therefore the total bending stiffness equals to only timber beam stiffness,  $EI_{to} = E_t I_t$ . The schematic distribution of bending stresses in all of the cases is displayed in Fig. 6.

The failure of the TCC beams in bending test is usually triggered by tensile failure of fibres located on the bottom of the section (LeBorgne & Gutkowski 2010; Yeoh et al. 2011b) and the stress-strain relationship of timber in tension is essentially linear up to the failure point. Accordingly, the ultimate loading capacity ( $P_u$ ) and corresponding ultimate deflection ( $\delta_u$ ) of the simply supported beam for different cases under four-point bending test can be calculated, respectively from

$$\left\{ \begin{array}{ll} P_u = \frac{8 EI_{fc} f_t}{E_t (2a_2 + h_t) (1 - \alpha) L} & \delta_u = \frac{(2 + 2\alpha - \alpha^2) f_t L^2}{12 E_t (2a_2 + h_t)} \quad : \text{Full-composite} \\ P_u = \frac{8 EI_{ef} f_t}{E_t (2a_2 + h_t) (1 - \alpha) L} & \delta_u = \frac{(2 + 2\alpha - \alpha^2) f_t L^2}{12 E_t (2a_2 + h_t)} \quad : \text{Semi-composite} \\ P_u = \frac{8 EI_{nc} f_t}{E_t h_t (1 - \alpha) L} & \delta_u = \frac{(2 + 2\alpha - \alpha^2) f_t L^2}{12 E_t h_t} \quad : \text{No-composite} \\ P_u = \frac{8 EI_{to} f_t}{E_t h_t (1 - \alpha) L} & \delta_u = \frac{(2 + 2\alpha - \alpha^2) f_t L^2}{12 E_t h_t} \quad : \text{Timber-only} \end{array} \right. \quad (15)$$

where  $f_t$ ,  $L$  and  $\alpha$  are the maximum tensile stress of timber (modulus of rupture), beam span and proportion of applied couple loads distance to total beam span, respectively.

## 4 COMPARATIVE STUDIES

### 4.1 Serviceability range

Four TCC beams tested by Khorsandnia et al. (2012) within serviceability range are analysed using developed FE models and manual calculation. The maximum size of elements in the 1D frame and continuum-based FE models is limited to 400 mm and 40 mm, respectively. The beams were subjected to 4-point bending and details of the beams including span, RC slab and timber beam dimensions, number and type of connection, applied load distance and the material properties (including compressive strength of concrete, moduli of elasticity and rupture of timber) are reported in Table 2. The geometry and material properties of the beams are within the same range, however, the number and type of connections are totally different. Therefore, the interaction behaviour between concrete and timber is different from sample to sample and that affects the global behaviour of TCC beams.

Table 2. The geometry and material properties of the beams are within the same range, however, the number and type of connections are totally different. Therefore, the interaction behaviour between concrete and timber is different from sample to sample and that affects the global behaviour of TCC beams.

Table 2. TCC beam details and material properties used in FE models and manual analysis in serviceability range.

Beam	Span (m)	Dimensions (mm)		Connection		Load Dis. (m)	Material Properties		
		RC Slab	Timber Beam	No.	Type		$f_{cp}$ Conc. (MPa)	MOE Tim. (GPa)	MOR Tim. (MPa)
B-NS (Khorsandnia et al. 2012)	5.8	600×75	250×48	12	NS	1.93	50.3	12.4	33.4
B-SFS (Khorsandnia et al. 2012)	5.8	600×75	250×48	16	SFS	1.93	50.3	12.3	33.4
B-4BM (Khorsandnia et al. 2012)	5.8	600×75	250×48	4	BM	1.93	50.3	13.2	33.4
B-6BM (Khorsandnia et al. 2012)	5.8	600×75	250×48	6	BM	1.93	50.3	13.5	33.4

The results of continuum-based and frame element FE models, respectively are denoted as FEM-CON and FEM-FR and shown in Fig. 7. Further, the results of manual calculations based on Full-composite, Semi-composite, No-composite and Timber-only behaviours are provided in Fig. 7. Based on the obtained results, the load-displacement behaviour of all TCC beams remains significantly linear within serviceability range which is in good agreement with analytical outcomes. Regarding the overall performance of the FE models within the serviceability range, it should be noted that

the stiffness of B-SFS, B-4BM and B-6BM beams have been underestimated compared to the experimental results, whereas for B-NS beam the stiffness has been overestimated by FE models. All TCC beams show semi-composite behaviour considering that the loading and unloading responses are between Full-composite and No-composite behaviours. Further, the comparison between experimental and analytical results indicates the sufficient accuracy of the developed FE models.

In Table 3, the load corresponding to 10 mm deflection and predicted ultimate loading capacity of each TCC beam are reported and compared with FE predictions and manual calculations. Based on the predicted results by FE models, B-NS has the minimum errors (FEM-CON = 0%, FEM-FR = 6% and Semi-comp. = 3%) compared to experimental result, whereas B-4BM has the greatest errors (FEM-CON = 31%, FEM-FR = 25% and Semi-comp. = 21%). Overall, the results of B-4BM and B-6BM beams are about 15-30% less than the experimental values. This may partly be due to the fact that friction between timber and concrete in the middle of the beams is ignored where there is no connection. It may also be a result of underestimating the load capacity of bird mouth connections. However, further investigations are recommended to understand the underlying reason for this discrepancy. Moreover, for the B-NS beam the ultimate loading capacity predicted by FE models is dramatically different than manual calculations, which is believed to be the result of allowing for the nonlinear behaviour of the connection in the FE model.

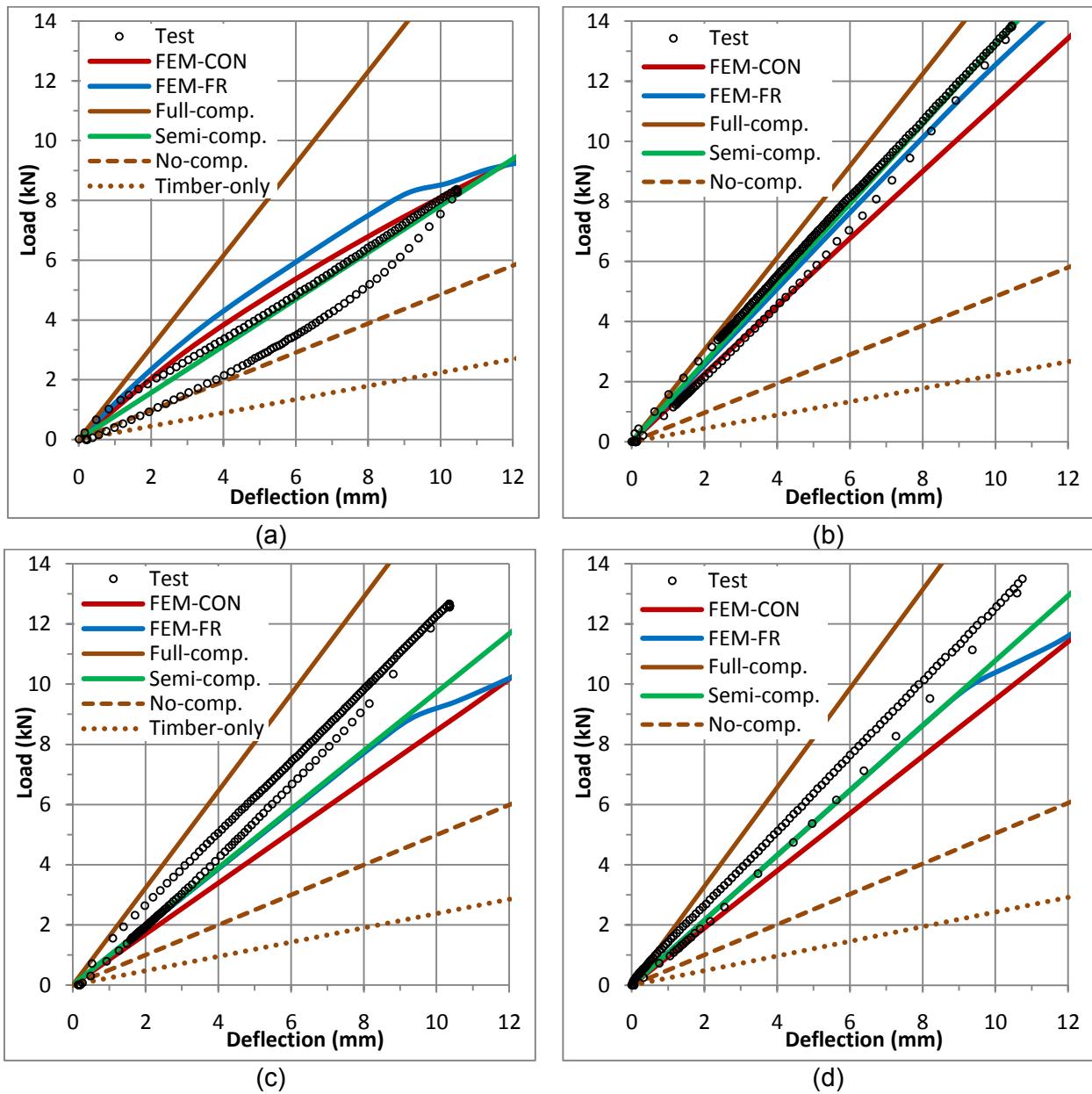


Fig. 7 Load versus deflection of (a) B-NS, (b) B-SFS, (c) B-4BM and (d) B-6BM beams for Khorsandnia et al. (2012) tests in serviceability range.

The average, standard deviation and coefficient of variation of different analytical models in serviceability range are reported in Table 4. Based on the results, all the models used for analysis of TCC beams under SLS loads have sufficient accuracy and they can adequately represent the global behaviour of the beam within this range. Among the different methods, manual calculation has the minimum error (9%) as well as the least variation (10.6%). Accordingly, in the cases considered in this study, using linear response based on Eurocode 5 provision can be sufficient for analysis of TCC beams within the serviceability range.

Table 3. Load corresponding to 10 mm deflection and predicted ultimate loading capacity obtained from experimental and analytical results in serviceability range.

Beam	Method	Load corr. to 10 mm def.		$P_u$ (kN)
		$P$ (kN)	$PIP(\text{test})$	
B-NS (Khorsandnia et al. 2012)	Test	8.04	-	-
	FEM-CON	8.07	1.00	29.98
	FEM-FR	8.52	1.06	28.54
	Full-comp.	15.39	1.91	53.78
	Semi-comp.	7.82	0.97	45.01
	No-comp.	4.85	0.60	37.41
	Timber-only	2.24	0.28	17.27
B-SFS (Khorsandnia et al. 2012)	Test	13.26	-	-
	FEM-CON	11.22	0.85	48.16
	FEM-FR	12.54	0.95	44.40
	Full-comp.	15.30	1.15	53.85
	Semi-comp.	13.21	1.00	52.19
	No-comp.	4.83	0.36	37.56
	Timber-only	2.22	0.17	17.27
B-4BM (Khorsandnia et al. 2012)	Test	12.28	-	-
	FEM-CON	8.46	0.69	40.05
	FEM-FR	9.17	0.75	37.81
	Full-comp.	16.11	1.31	53.22
	Semi-comp.	9.73	0.79	46.79
	No-comp.	4.99	0.41	36.26
	Timber-only	2.37	0.19	17.27
B-6BM (Khorsandnia et al. 2012)	Test	12.53	-	-
	FEM-CON	9.51	0.76	44.02
	FEM-FR	10.37	0.83	43.86
	Full-comp.	16.43	1.31	53.00
	Semi-comp.	10.79	0.86	47.68
	No-comp.	5.05	0.40	35.80
	Timber-only	2.43	0.19	17.27

Table 4. Average, standard deviation and coefficient of variation of FE and manual analyses in serviceability range.

Method	Ave.	Stan. Dev.	Coef. of Var.
FEM-CON	0.82	0.136	16.5%
FEM-FR	0.89	0.137	15.3%
Semi-comp.	0.91	0.096	10.6%

#### 4.2 Ultimate range

Five TCC beams from two different experimental programs (Clouston et al. 2005; Yeoh et al. 2011b) have been chosen from the literature to verify the accuracy of the developed FE models for capturing the full load-deflection and ultimate loading capacity. The geometrical details and adopted material properties for the TCC beams are summarized in Table 5. The span of the beams is within the range of 8-10 m. The

beams tested by Yeoh et al. (2011b) have T-shape section, whereas the beam in Clouston et al. (2005) test is rectangular. The considered beams have various numbers and types of connection and the shear-slip behaviour of connections are described in the previous section.

Table 5. TCC beam details and material properties used in FE models and manual analysis in ultimate range.

Beam	Span (m)	Dimensions (mm)		Connection		Load Dis. (m)	Material Properties		
		RC Slab	Timber Beam	No.	Type		$f_{cp}$ Conc. (MPa)	MOE Tim. (GPa)	MOR Tim. (MPa)
A1-R150 (Yeoh et al. 2011b)	8.0	600×65	400×63	6	R150	2.67	58.0	11.3	33.4
B1-R150 (Yeoh et al. 2011b)	8.0	600×65	400×63	10	R150	2.67	58.0	11.3	33.4
C1-T (Yeoh et al. 2011b)	8.0	600×65	400×63	10	T	2.67	54.4	11.3	33.4
E1-R300 (Yeoh et al. 2011b)	10.0	600×65	400×63	6	R300	3.33	48.2	11.3	33.4
Clouston et al. (2005)	9.86	960×120	960×220	3	Steel Mesh	2.60	30.0	11.5	20.0

The experimental load-deflection of Yeoh et al. (2011b) and Clouston et al. (2005) tests as well as the response captured by FE models and manual analyses are displayed in Figs. 8 and 9, respectively. In the developed FE models, the ultimate loading capacity of the TCC beams is governed by the tensile failure of the timber in the bottom layer which is typical failure mode in TCC beams as observed in the benchmark experimental results considered in this study (Clouston et al. 2005; Yeoh et al. 2011b). Most of the responses remain almost linear up to the failure point, however, some nonlinearities near the collapse load is observable (see Figs. 8 and 9) which should be taken into account when the accurate analysis of the beams required. The comparison between full-composite model, model with no-composite action and the test results shows that the beams have high composite efficiency that decreases near the failure load. The models based on FE and manual analysis can adequately represent the global behaviour (including stiffness and ultimate capacity) of TCC beams up to failure.

The ultimate loading capacity and the corresponding deflection at ultimate load obtained from experimental data and analytical results are given in

Table 6. Based on the results, all three analytical methods (continuum-based FE, frame element FE and manual analysis) can capture the ultimate loading capacity with reasonable accuracy. For capturing the ultimate deflection, however, the FE models have better accuracy than manual analysis and it was observed that using the serviceability stiffness ( $K_{s,0.4}$ ) for connections is an appropriate value to start with when the ultimate loading capacity of the TCC beams is being predicted.



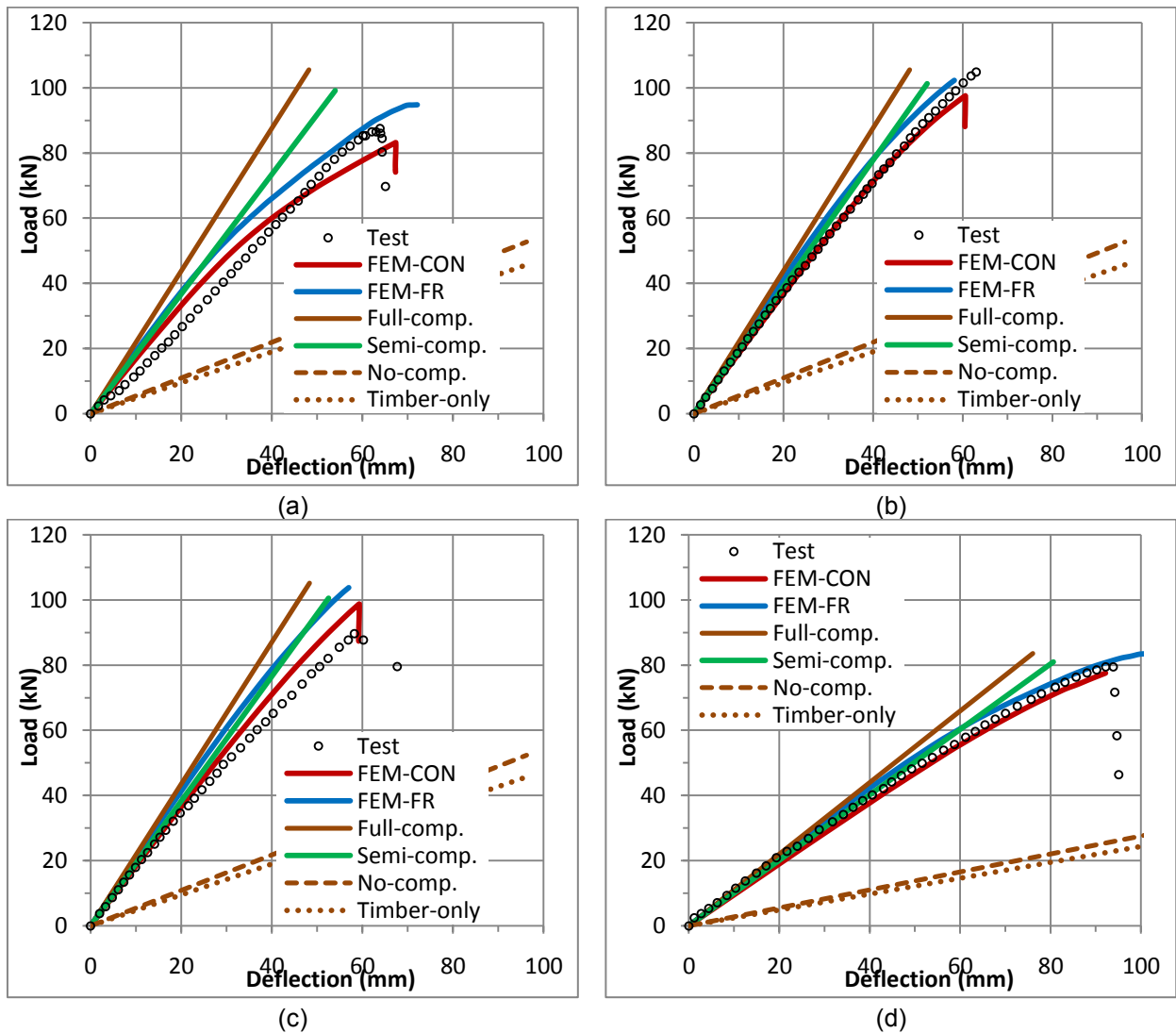


Fig. 8 Load versus deflection of (a) A1-R150, (b) B1-R150, (c) C1-T and (d) E1-R300 beams for Yeoh et al. (2012) tests in ultimate range.

The average, standard deviation and coefficient of variation for ultimate loading capacity and the corresponding deflection are calculated and provided in

Table 7. The developed continuum-based model can accurately capture both the ultimate loading capacity and its corresponding deflection (1% error) with maximum 6.8% variation, while the developed frame element model also offers good correlation with the experimental results (maximum 6% error with 8.6% variation). The accuracy in the manual analysis is not as good as for the FE models, particularly when the ultimate

deflection is concerned. It is also concluded that when the TCC beams have high composite efficiency, the global behaviour is almost linear up to failure and the nonlinear behaviour of timber and concrete does not have a significant influence on the response.

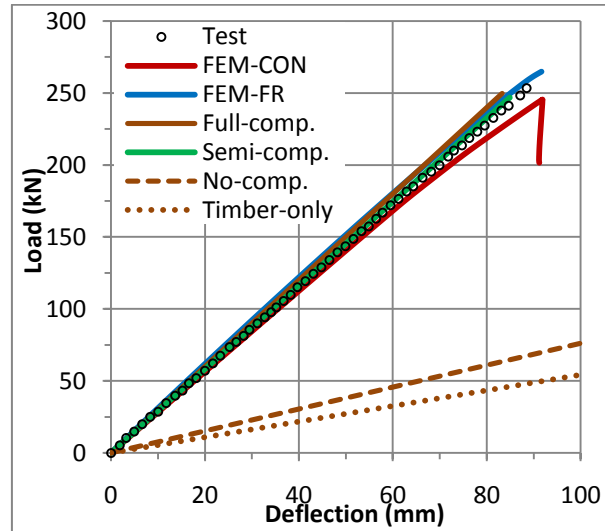


Fig. 9 Load versus deflection of Clouston et al. (2005) test in ultimate range.

## 5 CONCLUSIONS

This paper presents the short-term analytical response of timber-concrete composite structures with different methods. Two different types of finite element model, i.e. continuum-based and 1D frame fibre element, as well as procedures for manual calculations based on Eurocode 5 provision are developed and their details are discussed. Details of the FE models and the adopted constitutive laws for timber and concrete are provided and discussed. For modelling connections, application of nonlinear springs is introduced, which allows for the full load-slip behaviour of connections to be directly considered in the developed FE models. Furthermore, details of manual calculations according to Eurocode 5 are provided that captures four different types of behaviour including full-composite (no slip between timber and concrete), semi-composite (partial interaction between timber and concrete), no-composite (free slip between timber and concrete) and timber-only (without concrete slab). For verification of the developed models, three different experimental programs in serviceability and ultimate ranges with various TCC connections are chosen and the load-mid span deflection of the beams under four-point bending tests is compared to analytical results. Further, the load corresponding to 10 mm deflection in serviceability range and the ultimate loading capacity and its corresponding deflection in ultimate range are reported and the errors of each with respect to test results are calculated and reported.

The developed FE models, including continuum-based and 1D frame, can capture the short-term global behaviour of TCC beams under serviceability and ultimate loads

with sufficient accuracy. The ultimate capacity of all beams considered in this study is governed by tensile failure of timber in the bottom layer which is in good agreement

Table 6. Ultimate loading capacity and corresponding deflection obtained from experimental and analytical results in ultimate range.

Beam	Method	Ultimate Load		Ultimate Def.	
		$P_u$ (kN)	$P_u/P_u(\text{test})$	$\delta_u$ (mm)	$\delta_u/\delta_u(\text{test})$
A1-R150 (Yeoh et al. 2011b)	Test	87.52	-	63.92	-
	FEM-CON	83.19	0.95	67.35	1.05
	FEM-FR	94.81	1.08	72.14	1.13
	Full-comp.	105.53	1.21	48.17	0.75
	Semi-comp.	99.12	1.13	54.00	0.84
	No-comp.	52.69	0.60	96.21	1.51
	Timber-only	45.71	0.52	96.21	1.51
B1-R150 (Yeoh et al. 2011b)	Test	104.85	-	63.00	-
	FEM-CON	97.54	0.93	60.61	0.96
	FEM-FR	102.27	0.98	58.13	0.92
	Full-comp.	105.53	1.01	48.17	0.76
	Semi-comp.	101.26	0.97	52.05	0.83
	No-comp.	52.69	0.50	96.21	1.53
	Timber-only	45.71	0.44	96.21	1.53
C1-T (Yeoh et al. 2011b)	Test	89.67	-	58.22	-
	FEM-CON	98.75	1.10	59.26	1.02
	FEM-FR	103.80	1.16	57.03	0.98
	Full-comp.	105.16	1.17	48.34	0.83
	Semi-comp.	100.55	1.12	52.52	0.90
	No-comp.	52.35	0.58	96.21	1.65
	Timber-only	45.71	0.51	96.21	1.65
E1-R300 (Yeoh et al. 2011b)	Test	79.41	-	92.21	-
	FEM-CON	77.60	0.98	92.20	1.00
	FEM-FR	83.54	1.05	103.24	1.12
	Full-comp.	83.58	1.05	76.08	0.82
	Semi-comp.	81.00	1.02	80.61	0.87
	No-comp.	41.39	0.52	150.33	1.63
	Timber-only	36.57	0.46	150.33	1.63
Clouston et al. (2005)	Test	253.35	-	88.53	-
	FEM-CON	245.49	0.97	91.84	1.04
	FEM-FR	264.84	1.05	91.65	1.04
	Full-comp.	249.80	0.99	83.25	0.94
	Semi-comp.	246.88	0.97	84.92	0.96
	No-comp.	119.89	0.47	157.41	1.78
	Timber-only	85.33	0.34	157.41	1.78

Table 7. Average, standard deviation and coefficient of variation of FE and manual analyses in ultimate range.

Method	Ultimate Load			Ultimate Deflection		
	Ave.	Stan. Dev.	Coef. of Var.	Ave.	Stan. Dev.	Coef. of Var.
FEM-CON	0.99	0.067	6.8%	1.01	0.036	3.5%
FEM-FR	1.06	0.066	6.2%	1.04	0.089	8.6%
Semi-comp.	1.04	0.080	7.6%	0.88	0.052	5.9%

with the experimental data. Typically, the load-deflection response of TCC beams is almost linear line up to failure and this is due to high stiffness and strength of the connections utilised in this research program. Furthermore, using manual calculation based on Eurocode 5 in conjunction with tensile failure of timber can capture the serviceability and ultimate response of TCC beams with reasonable accuracy, provided the slip modulus of the connection is selected carefully (based on experimental data). For high stiffness connections, using serviceability slip modulus (characterised by a constant stiffness) it is possible to achieve accurate results particularly for the ultimate loading capacity. However, for connections with strongly nonlinear load-slip behaviour (e.g. normal screw), application of more advanced methods such as nonlinear FE is warranted.

## ACKNOWLEDGEMENTS

The authors would like to gratefully acknowledge the financial support of the Structural Timber Innovation Company (STIC) Research Consortium that has enabled this work to be undertaken.

## REFERENCES

- ABAQUS (2011), Ver. 6.11. Documentation edn, © Dassault Systèmes.
- Ahmadi, B.H. and Saka, M.P. (1993), "Behavior of Composite Timber-Concrete Floors" *Journal of Structural Engineering*, Vol. **119**(11), 3111-30.
- ANSYS (2011), Release 14.0 UP20111024 edn, SAS IP, Inc.
- Balogh, J., Fragiacomio, M., Gutkowski, R.M. and Fast, R.S. (2008), "Influence of Repeated and Sustained Loading on the Performance of Layered Wood-Concrete Composite Beams" *Journal of Structural Engineering*, Vol. **134**(3), 430-9.
- Branco, J.M., Cruz, P.J.S. and Piazza, M. (2009), "Experimental analysis of laterally loaded nailed timber-to-concrete connections" *Construction and Building Materials*, Vol. **23**(1), 400-10.
- Brunner, M., Romer, M. and Schnüriger, M. (2007), "Timber-concrete-composite with an adhesive connector (wet on wet process)" *Materials and Structures*, Vol. **40**(1),

119-26.

- CEB-FIP (1993), *CEB-FIP model code 1990: Design code*, Thomas Telford, London.
- Ceccotti, A. (1995), *Timber-Concrete Composite Structures*, Timber Engineering, Step 2, 1st Edn. (Centrum Hout, The Netherlands) E13/1-E13/12.
- Ceccotti, A., Fragiaco, M. and Giordano, S. (2006), "Long-term and collapse tests on a timber-concrete composite beam with glued-in connection" *Materials and Structures*, Vol. **40**(1), 15-25.
- CEN (1991), *Timber Structures - Joints made with mechanical fasteners - General principles for the determination of strength and deformation characteristics*. EN 26891, BSI, European Committee for Standardization, Brussels, Belgium.
- CEN (2008), *Eurocode 5: Design of timber structures - Part 1-1: General - Common rules and rules for buildings*. EN 1995-1-1:2004+A1, BSI, European Committee for Standardization, Brussels, Belgium.
- Clouston, P., Bathon, L.A. and Schreyer, A. (2005), "Shear and Bending Performance of a Novel Wood-Concrete Composite System" *Journal of Structural Engineering*, Vol. **131**(9), 1404-12.
- Clouston, P., Civjan, S. and Bathon, L. (2004), "Experimental behavior of a continuous metal connector for a wood-concrete composite system" *Forest Products Journal*, Vol. **54**(6), 76-84.
- Connors, T.E. (1989), "Segmented models for stress-strain diagrams" *Wood Science and Technology*, Vol. **23**(1), 65-73.
- Deam, B.L., Fragiaco, M. and Buchanan, A.H. (2008), "Connections for composite concrete slab and LVL flooring systems" *Materials and Structures*, Vol. **41**(3), 495-507.
- Dias, A.M.P.G., Lopes, S.M.R., Van de Kuilen, J.W.G. and Cruz, H.M.P. (2007a), "Load-Carrying Capacity of Timber-Concrete Joints with Dowel-Type Fasteners" *Journal of Structural Engineering*, Vol. **133**(5), 720-7.
- Dias, A.M.P.G., Van de Kuilen, J.W., Lopes, S. and Cruz, H. (2007b), "A non-linear 3D FEM model to simulate timber-concrete joints" *Advances in Engineering Software*, Vol. **38**(8-9), 522-30.
- Frangiaco, M. (2005), "A finite element model for long-term analysis of timber-concrete composite beams" *Structural Engineering and Mechanics*, Vol. **20**(2), 173-90.
- Frangiaco, M. (2012), "Experimental behaviour of a full-scale timber-concrete composite floor with mechanical connectors" *Materials and Structures*, 1-19.
- Frangiaco, M., Amadio, C. and Macorini, L. (2007), "Short- and long-term performance of the "Tecnaria" stud connector for timber-concrete composite beams" *Materials and Structures*, Vol. **40**(10), 1013-26.
- Gelfi, P., Giuriani, E. and Marini, A. (2002), "Stud Shear Connection Design for Composite Concrete Slab and Wood Beams" *Journal of Structural Engineering*, Vol. **128**(12), 1544-50.
- Glos, P. (1981), *Zur modellierung des festigkeitsverhaltens von bauholz bei druck-, Zug- und biegebeanspruchung*, Berichte zur zuverlässigkeitstheorie der bauwerke, SFB 96, Munich, Germany.
- Gutkowski, R., Brown, K., Shigidi, A. and Natterer, J. (2008), "Laboratory tests of composite wood-concrete beams" *Construction and Building Materials*, Vol. **22**(6), 1059-66.
- Gutkowski, R.M., Balogh, J. and To, L.G. (2010), "Finite-Element Modeling of Short-Term Field Response of Composite Wood-Concrete Floors/Decks" *Journal of Structural Engineering*, Vol. **136**(6), 707-14.
- Gutkowski, R.M., Brown, K., Shigidi, A. and Natterer, J. (2004), "Investigation of Notched Composite Wood-Concrete Connections" *Journal of Structural Engineering*, Vol. **130**(10), 1553-61.

- Hashin, Z. (1980), "Failure Criteria for Unidirectional Fiber Composites" *Journal of Applied Mechanics*, Vol. **47**(2), 329-34.
- Hashin, Z. and Rotem, A. (1973), "A Fatigue Failure Criterion for Fiber Reinforced Materials" *Journal of Composite Materials*, Vol. **7**(4), 448-64.
- Jorge, L.F., Lopes, S. and Cruz, H. (2011), "Interlayer influence on timber-LWAC composite structures with screw connections" *Journal of Structural Engineering*, Vol. **137**(5), 7.
- Khorsandnia, N., Valipour, H.R. and Crews, K. (2012), "Experimental and analytical investigation of short-term behaviour of LVL-concrete composite connections and beams" *Construction and Building Materials*, Vol. **37**(229-38).
- Khorsandnia, N., Valipour, H.R. and Crews, K. (2013), "Nonlinear finite element analysis of timber beams and joints using the layered approach and hypoelastic constitutive law" *Engineering Structures*, Vol. **46**(606-14).
- LeBorgne, M.R. and Gutkowski, R.M. (2010), "Effects of various admixtures and shear keys in wood-concrete composite beams" *Construction and Building Materials*, Vol. **24**(9), 1730-8.
- Lee, J. and Fenves, G.L. (1998), "Plastic-damage model for cyclic loading of concrete structures" *Journal of Engineering Mechanics*, Vol. **124**(8), 892.
- Lopes, S., Jorge, L. and Cruz, H. (2012), "Evaluation of non-linear behavior of timber-concrete composite structures using FE model" *Materials and Structures*, Vol. **45**(5), 653-62.
- Lublinter, J., Oliver, J., Oller, S. and Oñate, E. (1989), "A plastic-damage model for concrete" *International Journal of Solids and Structures*, Vol. **25**(3), 299-326.
- Lukaszewska, E., Fragiaco, M. and Johnsson, H. (2010), "Laboratory Tests and Numerical Analyses of Prefabricated Timber-Concrete Composite Floors" *Journal of Structural Engineering*, Vol. **136**(1), 46-55.
- Lukaszewska, E., Johnsson, H. and Fragiaco, M. (2008), "Performance of connections for prefabricated timber-concrete composite floors" *Materials and Structures*, Vol. **41**(9), 1533-50.
- Mackenzie-Helnwein, P., Eberhardsteiner, J. and Mang, H.A. (2003), "A multi-surface plasticity model for clear wood and its application to the finite element analysis of structural details" *Computational Mechanics*, Vol. **31**(1-2 SPEC.), 204-18.
- Mascia, N. and Soriano, J. (2004), "Benefits of timber-concrete composite action in rural bridges" *Materials and Structures*, Vol. **37**(2), 122-8.
- Ollgard, G., Slutter, G. and Fischer, W. (1971), "Shear strength of stud connectors in lightweight and normal weight concrete" *AISC Engineering Journal*, Vol. **8**(55-64).
- Schäfers, M. and Seim, W. (2011), "Investigation on bonding between timber and ultra-high performance concrete (UHPC)" *Construction and Building Materials*, Vol. **25**(7), 3078-88.
- Steinberg, E., Selle, R. and Faust, T. (2003), "Connectors for Timber-Lightweight Concrete Composite Structures" *Journal of Structural Engineering*, Vol. **129**(11), 1538-45.
- Valipour, H.R. and Bradford, M. (2012), "An efficient compound-element for potential progressive collapse analysis of steel frames with semi-rigid connections" *Finite Elements in Analysis and Design*, Vol. **60**(35-48).
- Valipour, H.R. and Bradford, M.A. (2009), "A steel-concrete composite beam element with material nonlinearities and partial shear interaction" *Finite Elements in Analysis and Design*, Vol. **45**(12), 966-72.
- Valipour, H.R. and Bradford, M.A. (2013), "Nonlinear P- $\Delta$  analysis of steel frames with semi-rigid connections" *Steel and Composite Structures*, Vol. **14**(1), 1-20.
- Yeoh, D., Fragiaco, M., De Franceschi, M. and Buchanan, A.H. (2011a), "Experimental tests of notched and plate connectors for LVL-concrete composite beams" *Journal of Structural Engineering*, Vol. **137**(2), 261-9.

Yeoh, D., Fragiacomio, M. and Deam, B. (2011b), "Experimental behaviour of LVL-concrete composite floor beams at strength limit state" *Engineering Structures*, Vol. **33**(9), 2697-707.